Progress In Electromagnetics Research C, Vol. 32, 27–41, 2012

FREQUENCY RECONFIGURABLE PLANAR INVERTED-F ANTENNA (PIFA) FOR CELL-PHONE APPLICATIONS

M.-J. Lee[1], Y.-S. Kim[1], and Y. Sung[2, *]

[1]Department of Radio Communication Engineering, Korea University, An-am dong 5-ga, Seoul 136-713, Korea

[2]Department of Electronics Engineering, Kyonggi University, Suwon-si, Gyeonggi-do, Korea

Abstract—In this paper, a frequency reconfigurable antenna for cell-phone applications is presented. The proposed structure is based on a conventional PIFA. In addition, two stubs, each with a varactor diode, are incorporated. In order to achieve the wideband characteristic, the first two resonant frequencies (f_1 and f_2) of the proposed antenna are controlled independently by the supplied voltages with the variation of the capacitances. The equivalent circuit of the varactor diode has been extracted in order to accurately predict the performance of the proposed antenna. In addition, parametric studies regarding the capacitance and antenna length have been conducted. The measurement results show that the proposed antenna has a tunable bandwidth defined by a VSWR < 2.5 of 45.7% (606 MHz $\sim$ 965 MHz) and 47.5% (1343 MHz $\sim$ 2181 MHz) at f_1 and f_2, respectively. Therefore, f_1 covers the LTE (698 MHz $\sim$ 798 MHz), CDMA (824 MHz $\sim$ 894 MHz), GSM (880 MHz $\sim$ 960 MHz) bands, and f_2 covers the DCS (1710 MHz $\sim$ 1880 MHz), PCS (1850 MHz $\sim$ 1990 MHz), WCDMA (1920 MHz $\sim$ 2170 MHz) bands. The measured average gains varied from -4.3 dBi to -1.5 dBi at f_1 and-6.4 dBi to -2.7 dBi at f_2.

1. INTRODUCTION

Recently, due to the various developments in communication systems, one device has come to perform many functions. For this reason, the broadband abilities and small size of the antenna are becoming more

Received 1 June 2012, Accepted 6 August 2012, Scheduled 9 August 2012

* Corresponding author: Yungje Sung (yjsung@kyonggi.ac.kr).

important. The planar inverted-F antenna (PIFA) has been developed because of its compactness and easy fabrication [1–4]. However, since the PIFA bandwidth is narrow, it has a drawback in a size reduction and a need for improving the antenna bandwidth. In order to address these issues, many multi resonances techniques have been developed using U-shaped or L-shaped slots, iterations, and additional strips [5–8]. In addition, meandered lines and shorting strips have been used to reduce the antenna size [9, 10]. Even so, there is a tradeoff between the antenna size and the operating bandwidth because the physical size has to be increased in order to create the additional resonances.

Reconfigurable antennas are an attractive structure due to their frequency extensibility without adding to the size of the antenna. Generally, reconfigurable antennas use a PIN diode to create multiple paths for the current [11–16]. As changing the state of the PIN diode, the additional current path was generated or the feeding point was switched. As a result, the bandwidth can be improved. However, this method has disadvantages in that the number of diodes is increased in order to create the additional resonances. For this reason, reconfigurable antennas using varactor diodes have been proposed because the electrical length of the antenna is simply varied by changing the applied bias [17–24]. In addition, the controllable impedance tuners using the varactor diodes were reported [25, 26]. Therefore, PIFAs utilizing varactor diodes have become an attractive solution in meeting the multiple resonance requirements of mobile applications [22–26]. However, the reported antennas had the complex structure and three or four diodes [25, 26]. The number of diode especially affects the consumption current and then, the operating time of battery. In the cell-phone engineer, it is very important factor, specially sleep mode. In addition, as increasing the number of diodes, the complexity of the bias circuit increases.

In this paper, a frequency reconfigurable PIFA for cell-phone applications is presented. The proposed PIFA has a dual-band operation. In order to reconfigure resonant frequencies, either the physical length or the capacitance of the antenna needs to be changed. Practically, it is difficult to change the physical size of an antenna. However, the capacitance can easily be changed through the use of varactor diodes. The frequency response of both bands can be tuned over a wide frequency range by changing the bias voltages of the varactor diodes. Furthermore, the resonant frequencies are lowered due to the parallel capacitances [18]. Until now, many reconfigurable antennas for cell-phone applications have been proposed. However, little information on reconfigurable antennas that cover six bands (LTE/CDMA/GSM/DCS/PCS/WCDMA) is currently available in the

Table 1. Antenna volume, covering the LTE band, and the diode type comparison with references.

	LTE band	diode type	volume	ratio (proposed antenna/[ref])
[14]	×	PIN diode	3010 mm^3	20.4%
[16]	×	PIN diode	2592 mm^3	23.7%
[22]	×	varactor	1166 mm^3	52.7%
[23]	×	varactor	926.3 mm^3	66.4%
[24]	×	varactor	1620 mm^3	40%
[29]	○	PIN diode	835.2 mm^3	73.6%

literature [29]. Moreover, although the proposed antenna can cover even the LTE band, it is quite small at only 615 mm^3. Table 1 shows the antenna volume, covering the LTE band or not, and diode type comparison with references. As shown in Table 1, the volume of the proposed antenna is smaller than that of references. In order to verify the tunability of the proposed structure, capacitance values have been altered using a high-frequency structure simulator (HFSS). In addition, the equivalent circuit of varactor diodes was extracted employing an advanced design systems (ADS) circuit simulator. By incorporating these results, a more accurate prediction of the performance of the antenna is possible [30]. In the actual measurement results, f_1 and f_2 cover the LTE/CDMA/GSM bands and the DCS/PCS/WCDMA bands based on a 2.5 : 1 VSWR, respectively.

2. ANTENNA DESIGN

2.1. Configuration and Parametric Studies of a PIFA

The geometry of the proposed antenna is depicted in Fig. 1. As shown in Fig. 1, the proposed structure has a radiating strip, shorting pin, and two stubs, each with a varactor diode. The varactor diodes are located on the stubs which have a fixed P_1 and P_2 from the feed and shorting pin connected directly to the ground plane and through a via hole; P_3 is the length of the radiating strip line placed on the top side. l_1 is the length of the stub placed on P_1 from the feed; l_2 is the length of the antenna excluding the ground plane; l_3 is the width of the antenna; s_l and s_r are the left and right length of space except for an antenna, respectively. w is the width of the microstrip line and g is the gap between the feed and the shorting pin. C_1 is the capacitor

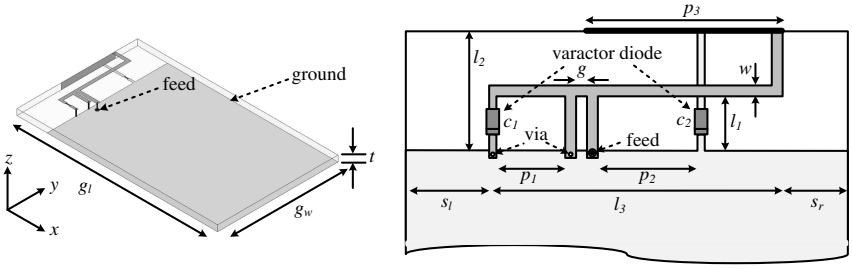

Figure 1. (a) General view and (b) details of the proposed antenna.

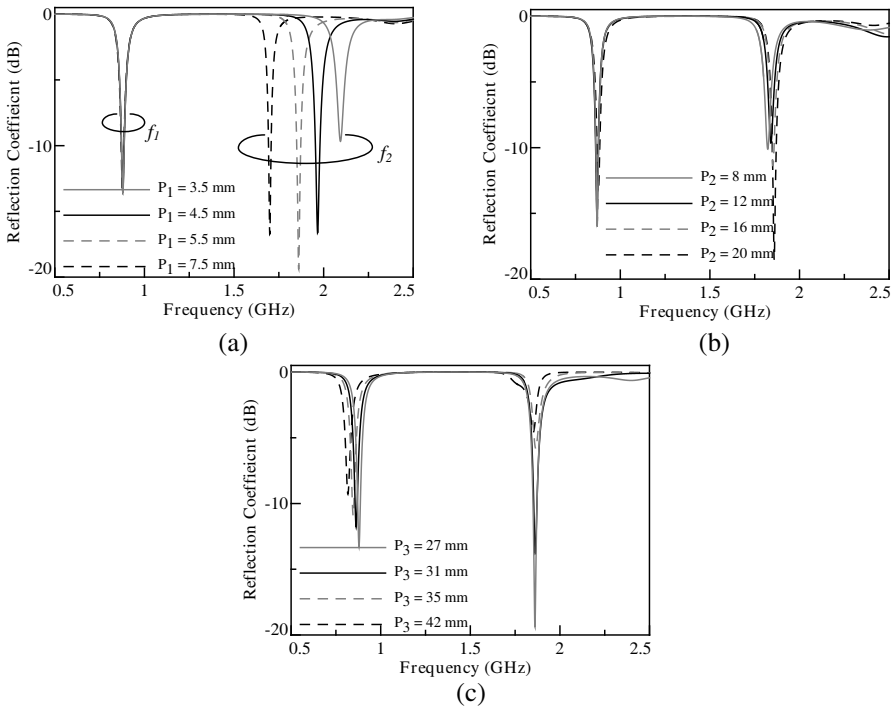

Figure 2. Simulated reflection coefficients as variation of the (a) P_1, (b) P_2, and (c) P_3. In these results, the capacitances are fixed for 0.5 pF.

of the stub placed at P_1 from the shorting pin; C_2 is the capacitor of the stub placed at P_2 from the feed. g_l and g_w are the total substrate length and width, respectively; t is the thickness of the substrate.

Figure 2 shows the simulated reflection coefficients as a variation of

the length of P_1, P_2 and P_3 whereas the capacitances are fixed at 0.5 pF. In the simulation, the antenna is designed to operate on a 1.574 mm thick dielectric substrate with permittivity of 2.2, and a total size of 60 mm × 120 mm. The other design parameters are: $P_1 = 5.5$ mm, $P_2 = 20$ mm, $P_3 = 27$ mm, $l_1 = 6$ mm, $l_2 = 11$ mm, $l_3 = 35.5$ mm, $s_l = 13.5$ mm, $s_r = 11$ mm and $g = 0.2$ mm. In addition, since the varactor diode cannot be applied in the HFSS, the varactor diode is replaced by a lumped capacitor. In Fig. 2, f_1 is slightly decreased by increasing the length of P_3; f_2 is decreased by increasing the length of P_1. The length of P_2, however, hardly affects. Further explanations about these characteristics will be illustrated in Fig. 3 and Fig. 4. Fig. 3 shows the electric field distributions at f_1 and f_2. The white region denotes the peak E-field, whereas the dark area has almost no E-field. Both plots have been normalized to the same minimum and maximum value. It is found from simulated result that the resonance path at f_1 is from the feed to the radiating strip. When the antenna resonates at f_1, the electric field is concentrated around the radiating strip. Therefore, the radiating strip can mainly affect the radiation performance at f_1. Meanwhile, it is found from simulated result that the resonance at f_2 is from the feed to the stub with C_1. When the electric field is concentrated around the shorter path, P_1, with C_1, the proposed antenna resonates at f_2. These results agree with previous parametric studies.

The simulated reflection coefficients, when changing the capacitance from 0.5 pF to 1.1 pF, are shown in Fig. 4. As presented in Fig. 4, f_1 and f_2 decrease as the capacitance value of C_1 and C_2 increase. These results show that the variation of the capacitance is more effective than changing the physical size of the antenna, and each resonant frequency can be operated independently by each capacitor. As shown in Fig. 4, the proposed antenna size can be reduced by high ca-

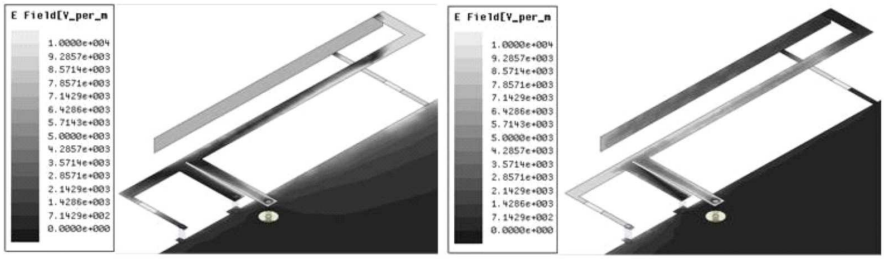

(a) (b)

Figure 3. Simulated electric field distributions according to the resonant frequency in (a) f_1 (0.87 GHz) and (b) f_2 (1.87 GHz).

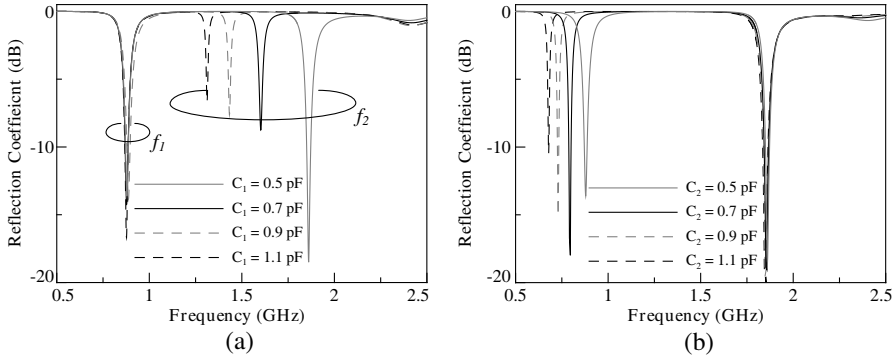

Figure 4. Simulated reflection coefficients as variation of the capacitance. In these results, another capacitance is fixed for 0.5 pF.

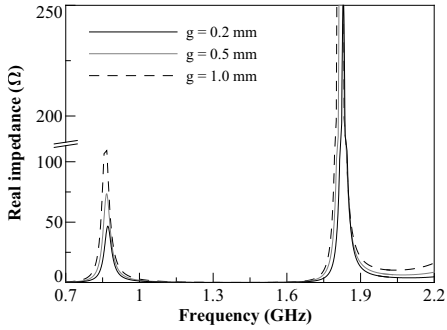

Figure 5. Simulated real impedances at the input as variation of the gap distance between the feed and shorting pin.

pacitance value. However, as decreasing the antenna size, the average gain is decreased. Therefore, there is a limitation for reducing the antenna size. In addition to these parameters, the gap distance between the feed and shorting pin, g, is an important factor. Although it can't change the resonant response, the input impedance of the antenna is affected by this gap. Fig. 5 shows the simulated real impedance at the input as a variation of the gap distance. As seen in the graph, a wider gap makes increases the real input impedance. This parameter can be used to change the input impedance without varying the resonant frequency.

2.2. Analysis of Varactor Diode

As shown in Section 2, a required capacitance range is small (0 pF $<$ C $<$ 2 pF). Although a larger capacitance makes the antenna have a lower

resonant frequency and smaller size, it causes a low radiation efficiency in the antenna. Therefore, the SMV 2019 made by Skyworks Corp. was selected. However, in order to apply the varactor diode to the proposed antenna, an analysis of the varactor diode is needed because the actual varactor diode has parasitic elements, i.e., capacitance and inductance.

Figure 6 shows the characteristics of the varactor diode. Fig. 6(a) shows the equivalent circuit of the varactor diode. In this circuit, L_p is the series inductance, and C_p is the parallel capacitance due to the varactor diode package or leads. R_s is the parallel resistance, a function of the applied voltage, and C_j is the junction capacitance that is also changed by the applied voltage. Fig. 6(b) shows the typical junction capacitance of the SMV2019. As shown in Fig. 6(b), the capacitance value changes from 2.25 pF to 0.17 pF as the applied voltage increases. Table 2 presents the extracted circuit elements of the varactor diode using the circuit simulator. Generally, the parasitic inductance of the SMV series is 1.5 nH, however, it is liable to change due to a periphery circuit or mounting condition. This is an important consideration, since R_s affects the antenna radiation performance. R_s decreases from 5.7 Ω to 2.2 Ω as the applied voltage increases. This means that the radiation loss of the lower resonant frequency is higher than at the higher resonant frequency. Unfortunately, 5.7 Ω is a very high value and may cause a noticeable reduction in the radiation efficiency [27].

Table 2. Extracted circuit elements of the varactor diode.

L_p	C_p	R_s	C_j
0.54 nH	0.17 pF	2.2 ∼ 5.7 Ω	0.17 ∼ 2.25 pF

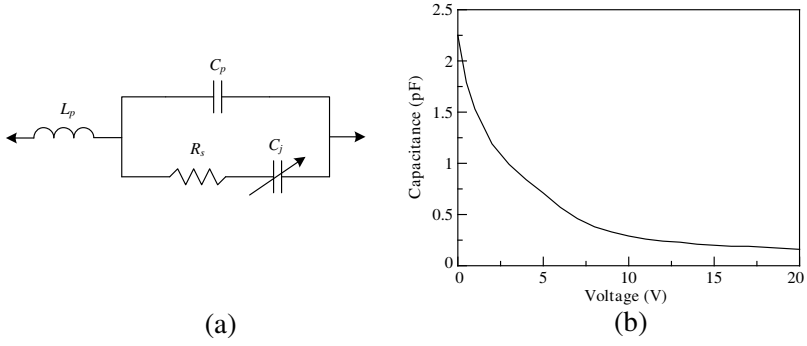

Figure 6. Characteristic of the varactor diode (from Skyworks Corp.). (a) Equivalent circuit and (b) typical junction capacitance values.

3. EXPERIMENTAL RESULTS

The photograph of the fabricated reconfigurable PIFA is shown in Fig. 7. The proposed antenna is designed on a 1.574 mm thick TLY-5 substrate with a dielectric constant of 2.2 and an overall ground size of 60 mm × 120 mm ($g_w \times g_l$). The distance P_1 between the shorting pin and capacitor C_1 is 5.5 mm and the distance P_2 between the feed and capacitor C_2 is 20.5 mm. The gap distance g between the shorting pin and the feed is 0.2 mm, the width of the strip line is 1.2 mm. The length of the stub connected to the ground plane, l_2, is 11 mm, and the other stub, l_1, is 6 mm. The length of the radiating strip line, P_3, is 27 mm and the width of the antenna, l_3, is 35 mm. The lengths of space except for antenna, s_l and s_r is 14 mm and 11 mm, respectively. The 82 pF lumped capacitor, used to prevent the current from the DC bias, is located between the shorting pin and ground plane, though this was not explained in the previous section. In order to measure the antenna performance, the bias-T of Picosecond Pulse Labs 5885 series was used. Using the bias-T, the VSWR and radiation patterns were measured without the bias circuit. Although this bias-T method can not control the individually applied voltages for the varactor diodes C_1 and C_2, it is helpful in verifying the correct antenna performance. The measurement set up configuration is shown in Fig. 8. It shows the configuration used to measure the VSWR, however, it is also applied to measure the radiation patterns. Using this measurement set up, the VSWR of the proposed antenna as a variation of the applied voltage was measured.

Figure 9 presents the VSWR measurement and simulation results. In the graph, V_1 and V_2 denote the supplied voltages to C_1 and C_2,

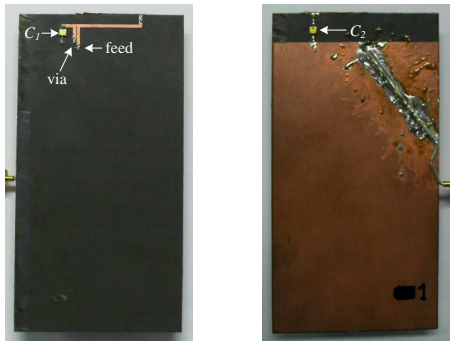

Figure 7. (a) Top view and (b) bottom view of the fabricated antenna.

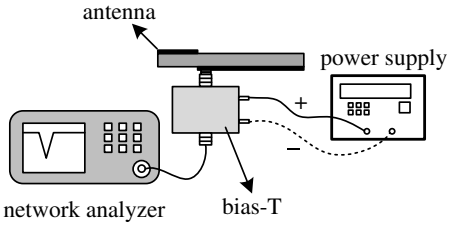

Figure 8. Configuration of the measurement set up.

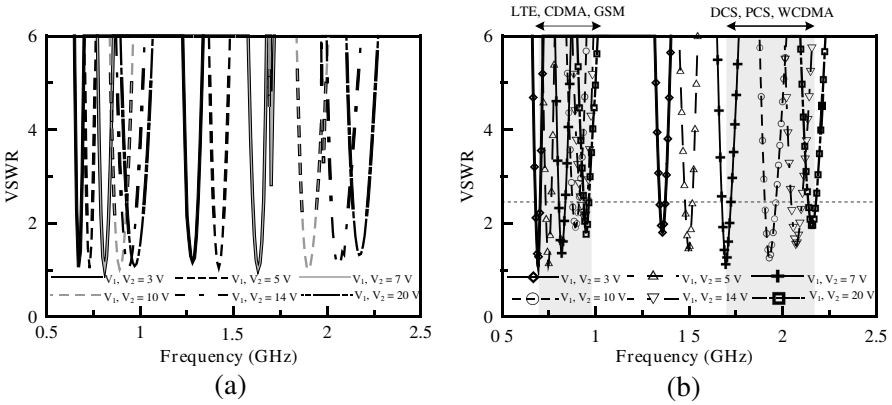

Figure 9. (a) Simulated result and (b) measured VSWR as variation of the applied voltage.

respectively. As mentioned previously, the capacitances of two varactor diodes are same, because the bias-T supplies the same voltage to each varactor diode, simultaneously. As shown in Fig. 9, the applied minimum voltage is 3 V because the varactor diodes have higher R_s at a lower voltage. Therefore, in order to reduce the radiation loss due to R_s, the minimum voltage is set to not 0 V but 3 V. By doing this, R_s is reduced by 1 Ω. The resonant frequency of the proposed antenna is increased by increasing the applied voltage because the capacitance of the varactor diode decreases. In the simulation results, since the parallel elements of the varactor diode are difficult to apply to the HFSS due to insufficient simulation results, the ADS is used in combination with the HFSS in order to obtain accurate simulation results [30]. The characteristics of the proposed structure without the varactor diode are extracted by the HFSS, and then the extracted data of HFSS are combined with the equivalent circuit of the varactor diode by ADS. This method reduces the simulation time because the full-wave simulation used to extract the physical layer data is conducted

only once. In the ADS, C_j and R_s are represented as applied voltages. In this graph, although the resonant frequencies when the lower value voltages are applied are slightly different from the measurement results, the higher resonant frequencies are nearly the same as the measurement results, and the frequency shift is clearly shown. According to the measurement results of the VSWR 2.5 : 1 specification, when the voltage is changed from 3 V to 20 V, the two resonant frequencies of the proposed antenna changed from 606 MHz to 965 MHz and from 1343 MHz to 2181 MHz, respectively. In addition, each fractional bandwidth (FBW) of the resonances at the lower and upper band is varied from 3.9% to 4.6% and from 2.1% to 3.21%, respectively. Therefore, the proposed antenna is able to cover the LTE, CDMA, GSM, DCS, PCS and WCDMA bands.

The measured average gain and radiation efficiency are shown in Fig. 10. As shown in these results, the average gain and radiation efficiency of the lower band are higher than that found for the upper band. The length of P_1, which determines the higher resonant frequency, is only $0.12\lambda_g$ at 1700 MHz, excluding the feeding line, however, the length from the feed to P_3, which determines the lower resonant frequency, is $0.2\lambda_g$ at 700 MHz, excluding the feeding line, and the radiating strip contributes to the radiation performance of f_1. As a result, the average gain and radiation efficiency at 1710 MHz are -6.4 dBi and 23%, respectively. In addition, since the lower voltage of the varactor diode has high R_s, the radiation performances around 700 MHz and 1700 MHz are not very good. However, as the frequency increased, the radiation performances increased to -2.7 dBi and 53%; the highest average gain is -1.5 dBi at 910 MHz with a radiation efficiency of 70%. The measured radiation patterns at the operating frequencies are shown in Fig. 11. The radiation patterns at 700 MHz and 880 MHz show an omni-directional pattern. In addition, since

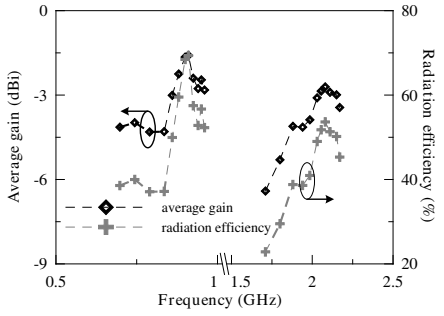

Figure 10. Measured average gain and radiation efficiency.

the radiation of the lower band is generated around the radiating strip line and C_2, the radiation patterns in the xy-plane are tilted. However, when the resonance of the antenna is generated at the higher frequencies, there are some nulls and dips that rapidly varied. Since the operating wavelengths become a short compared to the ground plane, surface current nulls are excited on the ground plane as a part of the

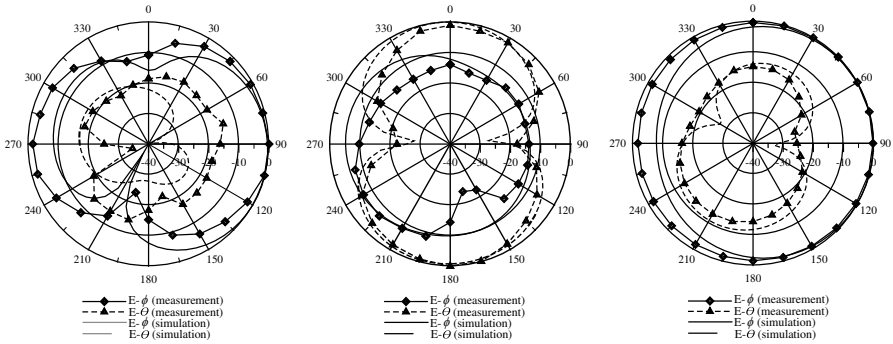

(a)

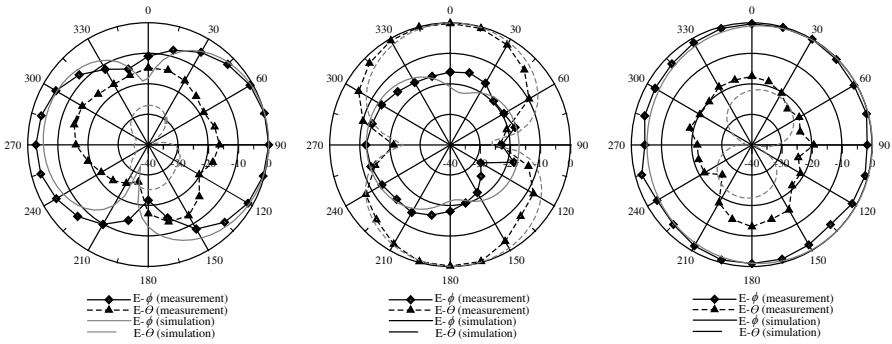

(b)

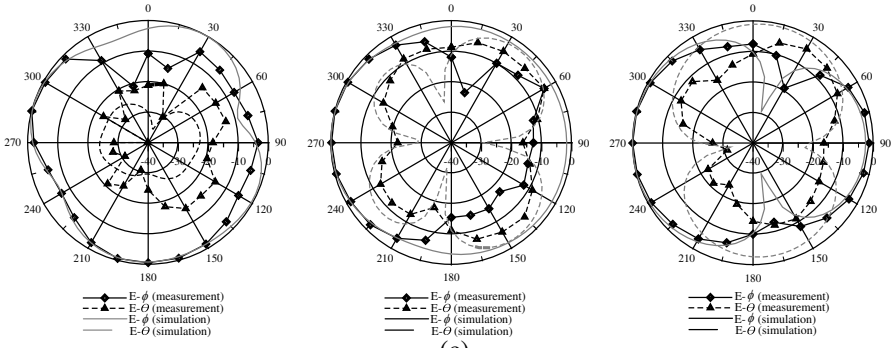

(c)

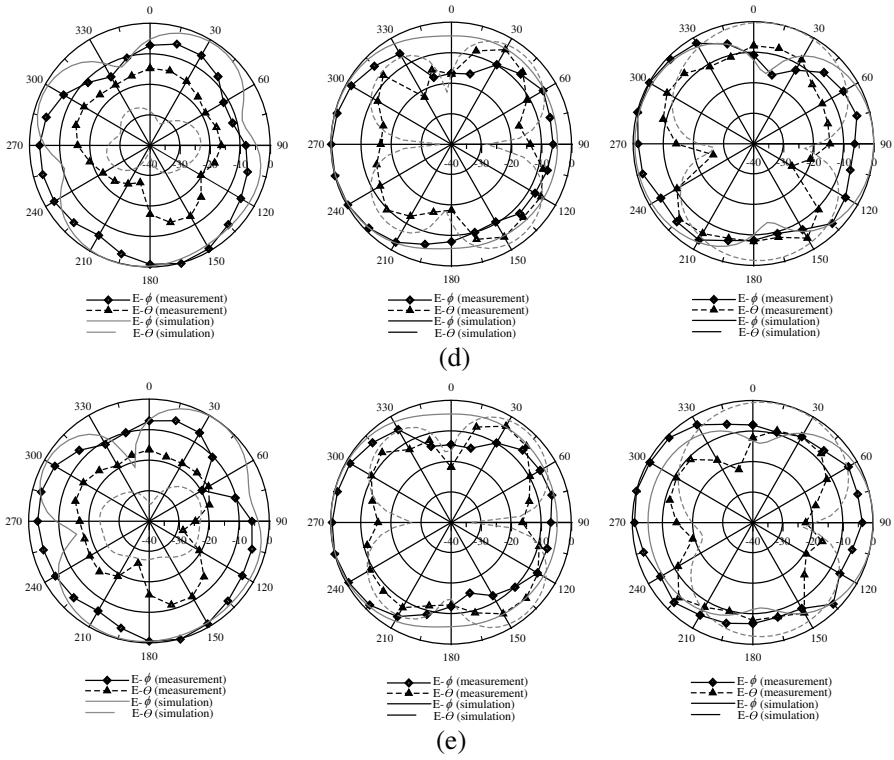

Figure 11. Measured radiation patterns in the xy-, zx-, and zy-planes, respectively at (a) 700 MHz (LTE), (b) 880 MHz (CDMA, GSM), (c) 1800 MHz (DCS), (d) 1930 MHz (PCS), and (e) 2070 MHz (WCDMA).

radiator [28]. Therefore, the radiation patterns in the xy-plane are titled towards the ground plane, however, they kept a similar pattern shape as the resonant frequency varied. Although slight differences between the measurement and simulation results are shown due to the position in the chamber, they are agreed closely.

4. CONCLUSION

In this paper, a frequency reconfigurable PIFA for cell-phone applications is presented. The proposed antenna has a dual-band based on two resonant paths. By using two varactor diodes, the frequency tunable response of both bands is achieved. The equivalent circuit of the varactor diode was extracted by a circuit simulator and applied to

predict the frequency response. The realized antenna was measured and analyzed under a bias-T condition. Although the antenna is designed to change both bands simultaneously, the required bands are individually obtained according to need. Since the proposed antenna is compact and has the wide frequency tunability, it can be used in mobile communication systems covering LTE, CDMA, GSM, DCS, PCS and WCDMA.

ACKNOWLEDGMENT

This research was supported by Basic Science Research Program through the National Research Foundation of Korea (NRF) funded by the Ministry of Education, Science and Technology (2010-0003396) and Industry Core Technology Development Project by the Ministry of Knowledge Economy.

REFERENCES

1. Rowell, C. R. and R. D. Murch, "A capacitively loaded PIFA for compact PCS handsets," *Proc. IEEE APS-Int. Symp.*, 742–745, Baltimore, MD, Jul. 1996.
2. Lui, G. K. H. and R. D. Murch, "Compact dual-frequency PIFA design using LC resonators," *IEEE Trans. Antennas Propag.*, Vol. 49, No. 7, 1016–1019, Jul. 2001.
3. Gao, Y., C. C. Chiau, X. Chen, and C. G. Parini, "A modified PIFA with a small ground plane," *Proc. IEEE AP-S Int. Symp.*, 515–518, Washongton DC, NY, Jul. 2005.
4. Sim, C.-Y.-D., "Dual and triple-band PIFA desigh for WLAN applications," *Microwave Opt. Technol. Lett.*, Vol. 49, No. 9, 2159–2162, Sep. 2007.
5. Nashaat, D. M., H. A. Elsadek, and H. Ghali, "Single feed compact quad-band PIFA antenna for wireless communication applications," *IEEE Tans. Antennas Propag.*, Vol. 53, No. 8, 2631–2635, Aug. 2005.
6. Liu, Z. D., P. S. Hall, and D. Wake, "Dual-frequency planar inverted-F antenna," *IEEE Trans. Antennas Propag.*, Vol. 45, No. 10, 1451–1458, Oct. 1997.
7. Saidatual, N. A., A. A. H. Azremi, R. B. Ahmad, P. J. Soh, and F. Malek, "Multiband fractal planar inverted F antenna (F-PIFA) for mobile phone application," *Progress In Electromagnetics Research B*, Vol. 14, 127–148, 2009.

8. Low, J. S. and C.-Y. Ai, "Experimental studies of a slot-loaded triangular folded planar inverted-F antenna," *Microwave Opt. Technol. Lett.*, Vol. 39, No. 5, 404–406, Dec. 2003.
9. Chen, H. T., K.-L. Wong, and T.-T. Chiou, "PIFA with a meandered and folded patch for the dual-band mobile phone application," *IEEE Trans. Antennas Propag.*, Vol. 51, No. 9, 2468–2471, Sep. 2003.
10. Chan, P. W., H. Wong, and E. K. N. Yung, "Wideband planar inverted-F antenna with meandering shorting strip," *Electron. Lett.*, Vol. 44, No. 6, 395–396, Mar. 2008.
11. Roscoe, D. J., L. Shafai, A. Ittipiboon, M. Cuhaci, and R. Douville, "Tunable dipole antennas," *Proc. IEEE AP-S Int. Symp.*, 672–675, Ann Arbor, MI, Jul. 1993.
12. Ramadan, A. H., K. Y. Kabalan, A. El-Hajj, S. Khoury, and M. Al-Husseini, "A reconfigurable u-koch microstrip antenna for wireless applications," *Progress In Electromagnetics Research*, Vol. 93, 355–367, 2009.
13. Feldner, L. M., C. T. Rodenbeck, C. G. Christdoulou, and N. Kinzie, "Electrically small frequency-agile PIFA-as-a package for portable wireless devices," *IEEE Trans. Antennas Propag.*, Vol. 55, No. 11, 3310–3319, Nov. 2007.
14. Li, Y., Z. Zhang, W. Chen, Z. Feng, and M. F. Iskander, "A quadband antenna with reconfigurable feedings," *IEEE Antenna Wireless Propag. Lett.*, Vol. 8, 1069–1071, 2009.
15. Lee, K.-M., Y.-J. Sung, J. W. Baik, and Y. S. Kim, "A tunable triangular microstrip patch antenna for multiband applications," *Microwave Opt. Technol. Lett.*, Vol. 51, No. 7, 1788–1790, Jul. 2009.
16. Wu, J., C. J. Panagamuwa, P. McEvoy, J. C. Vardaxoglou, and O. A. Saraereh, "Switching a dual band PIFA to operate in four bands," *Proc. IEEE AP-S Int. Symp.*, 2675–2678, Albuquerque, NM, Jul. 2006.
17. Shynu, S. V., G. Augustin, C. K. Aanandan, P. Mohanan, and K. Vasudevan, "Design of compact reconfigurable dual frequency microstrip antennas using varactor diodes," *Progress In Electromagnetics Research*, Vol. 60, 197–205, 2006.
18. Behdad, N. and K. Sarabandi, "A varactor-tuned dual-band slot antenna," *IEEE Trans. Antennas Propag.*, Vol. 54, No. 2, 401–408, Feb. 2006.
19. Behdad, N. and K. Sarabandi, "Dual-band reconfigurable antenna with a very wide tunability range," *IEEE Trans. Antennas*

Propag., Vol. 54, No. 2, 409–416, Feb. 2006.

20. Yang, S.-L. S., A. A. Kishk, and K. F. Lee, "Frequency reconfigurable u-slot microstrip patch antenna," *IEEE Antenna Wireless Propag. Lett.*, Vol. 7, 127–129, 2008.
21. White, C. R. and G. M. Rebeiz, "A shallow varactor-tuned capacity-backed slot antenna with a 1.9 : 1 tunning range," *IEEE Trans. Antennas Propag.*, Vol. 58, No. 3, 633–639, Mar. 2010.
22. Liang, J. and H. Y. D. Yang, "Varactor loaded tunable printed PIFA," *Progress In Electromagnetics Research B*, Vol. 15, 113–131, 2009.
23. Nguyen, V.-A., R.-A. Bhatti, and S.-O. Park, "A simple PIFA-based tunable internal antenna for personal communication handsets," *IEEE Antenna Wireless Propag. Lett.*, Vol. 7, 130–133, 2008.
24. Lim, J.-H., G.-T. Back, Y.-I. Ko, C.-W. Song, and T. Y. Yun, "A reconfigurable PIFA using a switchable PIN-diode and fine tuning varactor for USPCS/WCDMA/m-Wimax/WLAN," *IEEE Trans. Antennas Propag.*, Vol. 58, No. 7, 2404–2411, Jul. 2010.
25. Zhou, Z. and K. L. Melde, "Frequency agility of broadband antennas integrated with a reconfigurable RF impedance tuner," *IEEE Antenna Wireless Propag. Lett.*, Vol. 6, 56–59, 2007.
26. Melde, K. L., H.-J. Park, H.-H. Yeh, B. Fankem, Z. Zhou, and W. R. Eisenstadt, "Software defined match control circuit integrated with a planar inverted F antenna," *IEEE Trans. Antennas Propag.*, Vol. 58, No. 12, 3884–3890, Dec. 2010.
27. Peroulis, D., K. Sarabandi, and L. P. B. Katehi, "Design of reconfigurable slot antennas," *IEEE Trans. Antennas Propag.*, Vol. 53, No. 2, 645–654, Feb. 2005.
28. Wong, K.-L., W.-Y. Chen, and T.-W. Kang, "On-board printed coupled-fed loop antenna in close proximity to the surroung ground plane for penta-band WWAN mobile phone," *IEEE Trans. Antennas Propag.*, Vol. 59, No. 3, 751–757, Mar. 2011.
29. Cho, J., C. W. Jung, and K. Kim, "Frequency-reconfigurable two-port antenna for mobile phone operating over multiple service bands," *Electron. Lett.*, Vol. 45, No. 20, 1099–1011, Sep. 2009.
30. Boyle, K. R. and P. G. Steeneken, "A five-band reconfigurable PIFA for mobile phones," *IEEE Trans. Antennas Propag.*, Vol. 55, No. 11, 3300–3309, Nov. 2007.